

On the Explicit Construction and Statistics of Calabi-Yau Flux Vacua

Joseph P. Conlon ¹ and Fernando Quevedo ²

*DAMTP, Centre for Mathematical Sciences,
Wilberforce Road, Cambridge, CB3 0WA, UK*

Abstract

We explicitly construct and study the statistics of flux vacua for type IIB string theory on an orientifold of the Calabi-Yau hypersurface $\mathbb{P}_{[1,1,2,2,6]}^4$, parametrised by two relevant complex structure moduli. We solve for these moduli and the dilaton field in terms of the set of integers defining the 3-form fluxes and examine the distribution of vacua. We compare our numerical results with the predictions of the Ashok-Douglas density $\det(-\mathcal{R} - \omega)$, finding good overall agreement in different regions of moduli space. The number of vacua are found to scale with the distance in flux space. Vacua cluster in the region close to the conifold singularity. Large supersymmetry breaking is more generic but supersymmetric and hierarchical supersymmetry breaking vacua can also be obtained. In particular, the small superpotentials and large dilaton VEVs needed to obtain de Sitter space in a controllable approximation are possible but not generic. We argue that in a general flux compactification, the rank of the gauge group coming from D3 branes could be statistically preferred to be very small.

¹e-mail: J.P.Conlon@damtp.cam.ac.uk

²e-mail: F.Quevedo@damtp.cam.ac.uk

Contents

| | | |
|----------|--|-----------|
| 1 | Introduction | 2 |
| 2 | General Framework | 4 |
| 2.1 | The Model | 4 |
| 2.2 | Fluxes, Periods and Moduli | 6 |
| 3 | Vacua Statistics | 11 |
| 3.1 | The Vicinity of $\psi = \phi = 0$ | 11 |
| 3.2 | The Vicinity of the Conifold Locus | 14 |
| 4 | Summary and Discussion | 18 |

1 Introduction

It has been claimed that the current status of string theory resembles that of particle physics in the early 1960's[1] in the sense that there are many experimental results but no organising principle. For string theory the place of the experiments is taken by the many explicit string vacua that have been constructed over the years. One desirable avenue towards understanding string theory involves the development and questioning of its basic principles. Another less ambitious but equally important program is to explore the large variety of string vacua with the hope of learning more about the structure of the theory and of finding some of its phenomenological and/or cosmological implications.

In the phenomenological direction there has been substantial progress through the construction of string vacua with properties very similar to the standard model[2]. In cosmological applications, concrete ways have been found to realise inflation within string theory [3]. Furthermore the construction and study of string vacua and their properties has played an important role over the years in the understanding of the theory itself, as exemplified by the discovery of T -duality [4], mirror symmetry [5] and S -duality [6]. Mirror symmetry provides probably the most direct example in the sense that even though there were several ideas about its existence, the actual realisation came only after a plot of many of the vacua was found to be essentially symmetric under the exchange of complex and Kähler structure moduli, thus providing ‘experimental’ evidence for this symmetry.

Whether we like it or not, the lack of a close experimental test of the theory and the large abundance of vacua suggest that a reasonable direction to pursue is to create a large database of string vacua as a temporary substitute for experimental results. This database may eventually be used to extract model-

independent features of string vacua that may be testable. It may also give us some further hints into the structure of the theory itself.

These issues have been recently clarified through the study of antisymmetric tensor flux compactifications [7, 8]. In the absence of these fluxes there were myriads of vacua, each with a large continuous degeneracy parametrised by the moduli of the compactification space. Turning on the fluxes substantially reduces this degeneracy by making it discrete, owing to the Dirac quantisation condition for the fluxes. The fluxes can fix the values of the moduli, which then belong to a discrete set determined by the allowed fluxes. This huge discrete degeneracy makes a statistical analysis suitable for the study of vacua. The stabilisation of the dilaton and complex structure moduli is relatively straightforward, but flux compactifications may also enable the construction of metastable vacua with positive cosmological constant with the Kähler structure moduli also stabilised as in the KKLT scenario [9, 10].

Even though the number of flux vacua appears to be enormous for a general Calabi-Yau manifold, there are a number of requirements that must be satisfied for these vacua to be acceptable. First, as the entire framework is founded on a weak coupling approximation, only solutions leading to values of $\text{Im } \tau \gg 1$, where $\tau = C_0 + ie^{-\phi}$ is the dilaton-axion field that measures the string coupling. The self-duality of type IIB under the $SL(2, \mathbb{Z})$ S -duality symmetry implies that any solution can be mapped to the fundamental domain. Having mapped solutions to this region we can then only trust values of the dilaton substantially greater than one. As we will discuss in section 2.2, this is expected to be naturally suppressed statistically, with the proportion of vacua with $\text{Im } \tau > \tau_0$ falling as $\frac{1}{\text{Im } \tau_0}$. Secondly, the fluxes may or may not break supersymmetry by themselves and it is of interest to know the value of the supersymmetry breaking scale for each model. This is more urgent if the models are embedded in the full KKLT scenario in which non-perturbative superpotentials are also included to fix the Kähler moduli³. In order to guarantee a volume sufficiently larger than the string scale and believe the four-dimensional effective field theory analysis, the value of the gravitino mass induced only by the fluxes has to be hierarchically small, a condition that is not straightforward to satisfy.

Recently, Douglas and collaborators have developed statistical techniques to study string vacua e.g.[14, 15, 16]. In particular, in [15], a general formula was proposed that captures the statistical nature of the vacua, in terms of a density given by $\det(-\mathcal{R} - \omega)$ where \mathcal{R} is the curvature two form and ω the Kähler two-form on moduli space. In [17] the validity of this formula was successfully tested in a one-modulus example.

³In the KKLT scenario, the combination of fluxes that themselves break supersymmetry with a non-perturbative superpotential results in a supersymmetric minimum. In this case supersymmetry is broken only after the introduction of anti D3-branes [9, 11], magnetic fluxes on D7 branes [12] or in other vacua of the complex structure moduli[13].

In this note we extend this analysis to a simple two-modulus compactification, corresponding to the three-fold realisable as a hypersurface in the weighted projective space $\mathbb{P}_{[1,1,2,2,6]}$. We turn on 3-form fluxes and use the techniques of Candelas *et al* [18, 19, 20] to compute the periods. This allows us to determine the superpotential for the dilaton and complex structure moduli fields. We use a Monte Carlo analysis to study the distribution of vacua in the vicinities of the Landau-Ginzburg and conifold regions of moduli space. We compute the Ashok-Douglas index and compare with our results, finding good general agreement. We also investigate the distribution of values of the dilaton field as well as the supersymmetry breaking scale.

While in the last stages of this project we received an article [21] that discusses the Ashok-Douglas density for the same Calabi-Yau without performing the numerical analysis.

2 General Framework

We here review the construction of the particular Calabi-Yau we study, and the calculation of its periods[19, 20]. Some explicit flux compactifications on this Calabi-Yau are also presented in [22].

2.1 The Model

There exist many Calabi-Yau manifolds that can be realised as hypersurfaces in weighted projective space. The weighted projective space $\mathbb{P}_{[k_0, k_1, k_2, k_3, k_4]}^4$ is defined by

$$(w_0, w_1, w_2, w_3, w_4) \equiv (\lambda^{k_0} w_0, \lambda^{k_1} w_1, \lambda^{k_2} w_2, \lambda^{k_3} w_3, \lambda^{k_4} w_4)$$

and has four complex dimensions. To obtain a space of three complex dimensions we restrict to the hypersurface $P(w_i) = 0$, where P is a polynomial in the w_i . The condition that such a hypersurface be Calabi-Yau is that $\deg(P) = \sum_{i=0}^4 k_i$. In this paper we will make use of the Calabi-Yau hypersurface in $\mathbb{P}_{[1,1,2,2,6]}^4$, which arises from

$$w_0^{12} + w_1^{12} + w_2^6 + w_3^6 + w_4^2 = 0. \quad (1)$$

We shall denote this manifold by \mathcal{M} . \mathcal{M} has $h^{1,1} = 2$ and $h^{2,1} = 128$. The number of complex structure moduli is determined by the number of monomial deformations of degree 12 that can be added to (1). There are two complex structure moduli that are particularly important, which we shall denote by ψ and ϕ . These perturb (1) to

$$P(w_i) = w_0^{12} + w_1^{12} + w_2^6 + w_3^6 + w_4^2 - 12\psi (w_0 w_1 w_2 w_3 w_4) - 2\phi (w_0^6 w_1^6) = 0. \quad (2)$$

Their significance is due to their survival in the mirror manifold \mathcal{W} , obtained by identifying points in \mathcal{M} related by the action of G , the maximal group of scaling

symmetries of (1). G here is $\mathbb{Z}_2 \times \mathbb{Z}_6^2$, and its action is represented by

$$\mathbb{Z}_2 : (w_1, w_4) \rightarrow (\alpha w_1, \alpha w_4) \text{ with } \alpha^2 = 1,$$

$$\mathbb{Z}_6 : (w_1, w_3) \rightarrow (\beta^5 w_1, \beta w_3) \text{ with } \beta^6 = 1,$$

$$\mathbb{Z}'_6 : (w_1, w_2) \rightarrow (\gamma^5 w_1, \gamma w_2) \text{ with } \gamma^6 = 1.$$

These manifestly leave equation (2) invariant. All other degree 12 deformations of equation (2) are not well defined on the mirror. As \mathcal{W} has $h^{1,1} = 128$ and $h^{2,1} = 2$, it is an example of a Calabi-Yau with two complex structure moduli. Both \mathcal{M} and \mathcal{W} develop a conifold singularity when $864\psi^6 + \phi = 1$. This condition follows from requiring $P(w_i) = \underline{\nabla}P(w_i) = 0$ with $\underline{\nabla}\underline{\nabla}P$ non-singular.

The Ashok-Douglas index density describes the statistics of the class of models described in [8], namely flux compactifications of type IIB orientifolds. To fit the above model into this framework, we embed it into an F -theory model with an orientifold limit according to Sen's prescription[23]. The corresponding elliptically fibered four-fold is the hypersurface in weighted projective space $\mathbb{P}^5_{[1,1,2,2,12,18]}$ with $\chi = 19728$. The associated tadpole cancellation condition then reads[24]:

$$N_{\text{D3}} + N_{\text{flux}} = \frac{\chi}{24} = 822 \equiv L. \quad (3)$$

Here N_{D3} is the net number of D3 branes and N_{flux} the contribution of the fluxes to the D3 brane charge,

$$N_{\text{flux}} = \frac{1}{(2\pi)^4 \alpha'^2} \int_{\mathcal{M}} H_3 \wedge F_3. \quad (4)$$

Here $H_3 = dB_2$ and $F_3 = dC_2$ are the NS-NS and R-R 3-forms respectively. To cancel tadpoles in a supersymmetric fashion we then require the fluxes to carry at most 822 units of D3-brane charge (this number as usual measures the amount of negative D3 brane charge coming from D7 branes and orientifolds, in the orientifold realisation of the model).

In the low-energy approximation, the moduli of the Calabi-Yau appear as scalar fields in a supergravity theory. The effective four-dimensional $\mathcal{N} = 1$ supersymmetric field theory is determined by the Kähler potential $K_T(\xi_p, \phi_i)$ and the superpotential $W(\phi_i)$, where ξ_p ($p = 1, \dots, h^{1,1}$) represent the Kähler moduli and ϕ_i ($i = 1, \dots, h^{2,1} + 1$) the dilaton and complex structure moduli. The tree-level Kähler potential takes the form

$$K_T(\xi_p, \phi_i) = \hat{K}(\xi_p) + K(\phi_i), \quad (5)$$

where \hat{K} is the Kähler potential for the Kähler moduli and K that for the dilaton and complex structure moduli. We will write an explicit expression for K in the next section. As for \hat{K} , the only information we need to provide is that it is of

the no-scale form, in the sense that $\hat{K}^{-1}{}^p{}_q \hat{K}^p \hat{K}_q = 3$ where p and q label the Kähler moduli.

The appropriate superpotential for non-vanishing fluxes was proposed by Gukov, Vafa and Witten [24] and takes the form

$$W = \int_{\mathcal{M}} (F_3 - \tau H_3) \wedge \Omega. \quad (6)$$

τ is the complex dilaton-axion field and Ω the holomorphic $(3,0)$ form for the Calabi-Yau \mathcal{M} .

The combination of the fact that W does not depend on the Kähler moduli and the no-scale structure of the Kähler potential implies that the effective scalar potential is simply given by

$$V = e^{K_T} \left(D_i W D_{\bar{j}} \bar{W} K_{i\bar{j}}^{-1} \right), \quad (7)$$

where $D_i W = \partial_i W + (\partial_i K) W$ (in Planck mass units). Therefore, to stabilise these fields at the minimum of the potential we need $D_i W = 0$. The Kähler moduli only appear in the potential in the e^{K_T} overall factor and are not fixed. We will omit these fields in the rest of this paper except for pointing out that the no-scale structure implies that the order parameter for supersymmetry breaking is

$$D_p W = (\partial_p \hat{K}) W. \quad (8)$$

Thus a non-vanishing value of the superpotential W implies supersymmetry breaking by the F -term of the Kähler structure moduli. Since a Kähler transformation $K \rightarrow K + f + \bar{f}$, $W \rightarrow e^{-f} W$ leaves the action invariant, the value of W can always be rescaled and a more appropriate, Kähler transformation invariant, measure of supersymmetry breaking is the gravitino mass, given by

$$m_{3/2}^2 = e^K |W|^2. \quad (9)$$

Notice that in the KKLT construction, a non-perturbative superpotential depending on these fields is added [9, 11], breaking the no-scale structure and fixing the Kähler moduli. Anti D3-branes (or magnetic fluxes on the D7-branes [12]) are introduced in order to lift the minimum of the potential to a positive value. This can certainly be done in the present model, but as we have nothing new to say in this respect we concentrate on the dependence of the theory on the dilaton and complex structure moduli, to which we now turn.

2.2 Fluxes, Periods and Moduli

For any Calabi-Yau 3-fold, the middle homology and cohomology are naturally expressed in terms of a symplectic basis. That is, there exists a basis of 3-cycles

A^a and B_b and a basis of 3-forms α_a and β^b (where $a, b = 1, 2 \dots (h^{2,1} + 1)$), such that in homology

$$\begin{aligned} A^a \cap B_b &= -B_b \cap A^a = \delta_b^a, \\ A^a \cap A^b &= B_a \cap B_b = 0, \end{aligned} \quad (10)$$

and

$$\int_{A^b} \alpha_a = - \int_{B_a} \beta^b = \delta_a^b, \quad (11)$$

$$\int_{\mathcal{M}} \alpha_a \wedge \beta^b = - \int_{\mathcal{M}} \beta^b \wedge \alpha_a = \delta_a^b. \quad (12)$$

Such a symplectic basis is only defined up to $Sp(2n, \mathbb{Z})$ transformations, as these preserve the symplectic intersection form. The periods are defined as the integral of the holomorphic 3-form Ω over these cycles,

$$\int_{A_a} \Omega = z^a, \quad \int_{B^b} \Omega = \mathcal{G}_a. \quad (13)$$

The periods are encapsulated in the period vector, $\Pi = (\mathcal{G}_1, \dots, \mathcal{G}_n, z_1, \dots, z_n)$, where $n = h^{2,1} + 1$. This inherits the holomorphic freedom of Ω and is defined up to holomorphic rescalings $\Omega \rightarrow f(\phi_i)\Omega$. Note that $\Pi = \Pi(\phi_i)$, where ϕ_i are the complex structure moduli of the Calabi-Yau.

Given the vector of periods $\Pi(\phi_i)$, the Kähler potential on complex structure moduli space is given by [25]

$$\begin{aligned} K(\tau, \phi_i) &= -\ln(-i(\tau - \bar{\tau})) - \ln\left(i \int \Omega \wedge \bar{\Omega}\right) \\ &= -\ln(-i(\tau - \bar{\tau})) - \ln(-i\Pi^\dagger \cdot \Sigma \cdot \Pi) \\ &\equiv K_\tau + K_\phi. \end{aligned} \quad (14)$$

where

$$\Sigma = \begin{pmatrix} 0 & \mathbf{1}_n \\ -\mathbf{1}_n & 0 \end{pmatrix}$$

and τ is the dilaton-axion. We can then compute the metric on moduli space,

$$g_{\alpha\bar{\beta}} = \partial_\alpha \partial_{\bar{\beta}} K, \quad (15)$$

and the Riemann and Ricci curvatures

$$\begin{aligned} R_{\mu\bar{\nu}\rho}^\lambda &= -\partial_{\bar{\nu}}(g^{\lambda\bar{\alpha}} \partial_\mu g_{\rho\bar{\alpha}}), \\ R_{\mu\bar{\nu}}^\lambda &= R_{\mu\bar{\nu}\lambda}^\lambda = -\partial_\mu \partial_{\bar{\nu}} \log(\det g). \end{aligned} \quad (16)$$

In terms of the periods, the Gukov-Vafa-Witten superpotential is

$$W = (2\pi)^2 \alpha' (f - \tau h) \cdot \Pi(\phi_i), \quad (17)$$

where $f = (f_1, \dots, f_6)$ and $h = (h_1, \dots, h_6)$ are integral vectors of fluxes along the cycles. The fluxes F_3 and H_3 are elements of $H^3(\mathcal{M}, \mathbb{Z})$ and satisfy the flux quantisation conditions

$$\frac{1}{(2\pi)^2 \alpha'} \int_{\Sigma^3} F \in \mathbb{Z}, \quad \frac{1}{(2\pi)^2 \alpha'} \int_{\Sigma^3} H \in \mathbb{Z}, \quad (18)$$

where Σ^3 is an arbitrary 3-cycle. The amount of $D3$ -brane charge carried by the fluxes is then

$$N_{flux} = f^T \cdot \Sigma \cdot h. \quad (19)$$

The stabilisation of the complex structure moduli ϕ_i is governed by the following equations

$$\begin{aligned} D_{\phi_i} W &= \partial_{\phi_i} W + (\partial_{\phi_i} K) W = 0, \\ D_{\tau} W &= \partial_{\tau} W + (\partial_{\tau} K) W = 0. \end{aligned} \quad (20)$$

Distinct choices of fluxes stabilise the complex structure moduli at discrete points in moduli space. As the total number of flux vacua is very large, the distribution of discrete flux vacua can be approximated by a continuous distribution. Treating the fluxes as non-quantised, Ashok and Douglas[15] derived a formula for an index that gives an estimate of the total number of vacua with $N_{flux} < L$ on a region \mathcal{X} of moduli space

$$I_{vac}(N_{flux} \leq L) = \frac{(2\pi L)^K (-1)^{\frac{K}{2}}}{\pi^{n+1} K!} \int_{\mathcal{X}} \det(-\mathcal{R} - \mathbf{1} \cdot \omega) \quad (21)$$

where ω is the Kähler form and \mathcal{R} the curvature two-form on moduli space. In formula (21) K is the number of cycles along which flux is wrapped and L the total available $D3$ -brane charge. In a comparison with numbers of explicit vacua, the constant prefactor is obviously not relevant.

We will now restrict to cases where the Calabi-Yau \mathcal{M} has two complex structure moduli. The region \mathcal{X} includes the dilaton-axion moduli space. The weighted vacuum density over the Calabi-Yau moduli space is then evaluated to be[26]

$$d\mu = g_{\tau\bar{\tau}} d\tau \wedge d\bar{\tau} \wedge \left(4\pi^2 c_2 - \det(g_{a\bar{a}}) d\psi^1 \wedge d\psi^{\bar{1}} \wedge d\psi^2 \wedge d\psi^{\bar{2}} \right), \quad (22)$$

where $g_{\tau\bar{\tau}} = -\frac{1}{(\tau - \bar{\tau})^2}$ and c_2 , the second Chern class of \mathcal{M} , is given by

$$c_2 = \frac{1}{8\pi^2} (\text{tr}(\mathcal{R} \wedge \mathcal{R}) - \text{tr}\mathcal{R} \wedge \text{tr}\mathcal{R}). \quad (23)$$

(22) may be rewritten as

$$d\mu = g_{\tau\bar{\tau}}d\tau \wedge d\bar{\tau} \wedge d\psi^1 \wedge d\psi^{\bar{1}} \wedge d\psi^2 \wedge d\psi^{\bar{2}} \left[\epsilon^{ab}\epsilon^{\bar{a}\bar{b}} (R_{a\bar{a}1}^1 R_{b\bar{b}2}^2 - R_{a\bar{a}2}^1 R_{b\bar{b}1}^2) - \det g_{a\bar{a}} \right]. \quad (24)$$

To evaluate both (20) and (22) we must obtain a knowledge the periods, which in general is a highly non-trivial task. However, the manifold defined by (2) is of a class that has been extensively studied. The relevant periods have been computed in [19, 20], following the classic treatment of the quintic[18], and we will borrow their results. For the Calabi-Yau described by the hypersurface

$$P = \sum_{j=0}^4 x_j^{d/k_j} - d\psi x_0 x_1 x_2 x_3 x_4 - \frac{d}{q_0} \phi x_0^{q_0} x_1^{q_1} x_2^{q_2} x_3^{q_3} x_4^{q_4} = 0, \quad (25)$$

the fundamental period in the large ψ region is given by

$$\varpi_f(\psi, \phi) = \sum_{l=0}^{\infty} \frac{(q_0 l!) (d\psi)^{-q_0 l} (-1)^l}{l! \prod_{i=1}^4 (\frac{k_i}{d} (q_0 - q_i) l)!} u_l(\phi), \quad (26)$$

where

$$u_l(\phi) = (D\phi)^l \sum_{n=0}^{\lfloor \frac{l}{D} \rfloor} \frac{l! \prod_{i=1}^4 (\frac{k_i}{d} (q_0 - q_i) l)! (-D\phi)^{-Dn}}{(l - Dn)! n! \prod_{i=1}^4 (\frac{k_i q_i}{q_0} n + \frac{k_i}{d} (q_0 - q_i) l)!}. \quad (27)$$

This is obtained by direct integration of Ω and satisfies the Picard-Fuchs equation. There are other independent solutions to the Picard-Fuchs equation having a logarithmic dependence on ψ . In total there are six independent solutions, one for each 3-cycle, and the actual periods are a linear combination of these.

The two regions of moduli space that will most interest us are the vicinities of the Landau-Ginzburg point $\psi = \phi = 0$ and the the conifold locus $864\psi^6 + \phi = 1$. To obtain a basis of periods in the small ψ region, we analytically continue (26) to obtain

$$\varpi_f(\psi, \phi) = -\frac{2}{d} \sum_{n=1}^{\infty} \frac{\Gamma(\frac{2n}{d}) (-d\psi)^n u_{-\frac{2n}{d}}(\phi)}{\Gamma(n) \Gamma(1 - \frac{n}{d} (k_1 - 1)) \Gamma(1 - \frac{k_2 n}{d}) \Gamma(1 - \frac{k_3 n}{d}) \Gamma(1 - \frac{k_4 n}{d})}. \quad (28)$$

Here $u_\nu(\phi)$ is related to the hypergeometric functions and is defined through the contour integral

$$u_\nu(\phi) = \frac{2^\nu}{\pi} \int_{-1}^1 \frac{d\zeta}{\sqrt{1 - \zeta^2}} (\phi - \zeta)^\nu. \quad (29)$$

The contour integral is initially defined for $\text{Im}(\phi) > 0$ and then defined over the rest of the plane by deforming the integral contour. The branch cuts, which are unavoidable when ν is non-integral, start at ± 1 and run to $\pm\infty$.

We may derive a basis of periods from the fundamental period in a simple manner. If we define

$$\varpi_j(\psi, \phi) = \frac{-(2\pi i)^3}{\psi} \varpi_f(\alpha^j \psi, \alpha^{jq_0} \phi) \quad (30)$$

then $\varpi(\psi, \phi) = (\varpi_0(\psi, \phi), \varpi_1(\psi, \phi), \varpi_2(\psi, \phi), \varpi_3(\psi, \phi), \varpi_4(\psi, \phi), \varpi_5(\psi, \phi))$ gives a basis of periods known as the Picard-Fuchs basis. Naively (30) would seem to give 12 independent periods, but there are interrelations discussed in [19]. The net result is that, as expected, there are six independent periods. This basis is however not symplectic. A symplectic basis is given by

$$\Pi(\psi, \phi) = m \cdot \varpi(\psi, \phi). \quad (31)$$

Here m was computed in [22] and is given by

$$m = \begin{pmatrix} -1 & 1 & 0 & 0 & 0 & 0 \\ \frac{3}{2} & \frac{3}{2} & \frac{1}{2} & \frac{1}{2} & -\frac{1}{2} & -\frac{1}{2} \\ 1 & 0 & 1 & 0 & 0 & 0 \\ 1 & 0 & 0 & 0 & 0 & 0 \\ -\frac{1}{2} & 0 & \frac{1}{2} & \frac{1}{2} & 0 & 0 \\ \frac{1}{2} & \frac{1}{2} & -\frac{1}{2} & \frac{1}{2} & -\frac{1}{2} & \frac{1}{2} \end{pmatrix}.$$

In principle, equation (31) completely determines the periods near $\psi = 0$. However, it involves the integral expression (29) for $u_\nu(\phi)$ which is inconvenient for a computational treatment. Such a treatment is facilitated by the power series expansion of $u_\nu(\phi)$ in the small ϕ region found in [19]. This is given by

$$u_\nu(\phi) = \frac{e^{\frac{i\pi\nu}{2}} \Gamma\left(1 + \frac{\nu(k_1-1)}{2}\right)}{2\Gamma(-\nu)} \sum_{m=0}^{\infty} \frac{e^{i\pi m/2} \Gamma\left(\frac{m-\nu}{2}\right) (2\phi)^m}{m! \Gamma\left(1 - \frac{m-\nu k_1}{2}\right)} \quad (32)$$

The region of convergence of equations (28), (29), and (32) is worth discussing. We will here be specific to the particular Calabi-Yau described in section 2. This manifold develops a conifold singularity when $\phi + 864\psi^6 = \pm 1$ and there is also a strong coupling singularity when $\phi = \pm 1$. The regions of convergence are determined by the singularities. All three equations are only valid for $|\frac{864\psi^6}{\phi \pm 1}| < 1$ and equation (32) has the additional restriction $|\phi| < 1$.

We will also be interested in the periods near the conifold locus. As will be further discussed in section (3.2), the periods here have a certain standard form. However, for their exact numerical determination, we will use the neolithic approach, directly evaluating the power series (31) near the conifold locus.

Finally, the Calabi-Yau we work on is the original manifold \mathcal{M} defined by the locus of the polynomial (2), and not its mirror \mathcal{W} . \mathcal{M} has a total of 128 complex structure moduli. We expect some to be removed by the orientifold

symmetry, but there will still be many which we are ignoring. The validity of this was explained in [22]. The group G is a symmetry of (2) and if we only turn on fluxes invariant under this symmetry then the superpotential can only have a higher-order dependence on the other moduli. It is thus consistent to set all other moduli equal to zero and focus only on the moduli in equation (2) and their associated fluxes. We will comment briefly on the general situation in the last section.

3 Vacua Statistics

The two natural regions for testing the Ashok-Douglas formula are the vicinities of the Landau-Ginzburg point $\psi = \phi = 0$ and the conifold locus $864\psi^6 + \phi = 1$.

3.1 The Vicinity of $\psi = \phi = 0$

A symplectic basis for the periods was given in equation (31). Let us untangle this in the vicinity of $\psi = 0$. We can expand $\Pi(\psi, \phi)$ as

$$\Pi = \underline{a}(\phi) + \underline{b}(\phi)\psi^2 + \underline{c}(\phi)\psi^4 + \mathcal{O}(\psi^6). \quad (33)$$

Here $\underline{a}, \underline{b}$ and \underline{c} are vector functions of ϕ whose explicit form arises from the combination of equations (28), (32), (30) and (31). It can be checked that $\underline{a}^\dagger \cdot \Sigma \cdot \underline{b} = \underline{a}^\dagger \cdot \Sigma \cdot \underline{c} = 0$, implying

$$\Pi^\dagger \cdot \Sigma \cdot \Pi = (\underline{a}^\dagger \cdot \Sigma \cdot \underline{a}) + (\underline{b}^\dagger \cdot \Sigma \cdot \underline{b})\psi^2\bar{\psi}^2 + \mathcal{O}(|\psi|^6),$$

and consequently

$$\begin{aligned} K_\phi(\psi, \phi) &= -\ln(-i\Pi^\dagger \cdot \Sigma \cdot \Pi) \\ &= -\ln(-i\underline{a}^\dagger \cdot \Sigma \cdot \underline{a}) - \ln\left(1 + \frac{(\underline{b}^\dagger \cdot \Sigma \cdot \underline{b})}{(\underline{a}^\dagger \cdot \Sigma \cdot \underline{a})}\psi^2\bar{\psi}^2 + \mathcal{O}(|\psi|^6)\right) \\ &= -\ln(-i\underline{a}^\dagger \cdot \Sigma \cdot \underline{a}) - \frac{(\underline{b}^\dagger \cdot \Sigma \cdot \underline{b})}{(\underline{a}^\dagger \cdot \Sigma \cdot \underline{a})}\psi^2\bar{\psi}^2 + \mathcal{O}(|\psi|^6). \end{aligned} \quad (34)$$

Equations (20) then have the form

$$\frac{1}{\psi}D_\psi W = 0 \Rightarrow (f - \tau h) \cdot (\underline{\alpha}_1(\phi) + \underline{\alpha}_2(\phi)\psi^2 + \underline{\alpha}_3(\phi)\bar{\psi}^2) = 0, \quad (35)$$

$$D_\phi W = 0 \Rightarrow (f - \tau h) \cdot (\underline{\beta}_1(\phi) + \underline{\beta}_2(\phi)\psi^2) = 0, \quad (36)$$

$$D_\tau W = 0 \Rightarrow (f - \bar{\tau}h) \cdot (\underline{a}(\phi) + \underline{b}(\phi)\psi^2) = 0, \quad (37)$$

where we have dropped terms of $\mathcal{O}(|\psi|^4)$. Here $\underline{\alpha}(\phi)$ and $\underline{\beta}(\phi)$ are complicated functions of ϕ depending on the integral expressions for $u_\nu(\phi)$. However, when

$|\phi| < 1$ the use of the power series expansion in equation (32) converts $\underline{\alpha}(\phi)$ and $\underline{\beta}(\phi)$ to a more tractable form. The leading behaviour of the metric $g_{\alpha\bar{\beta}} = \partial_\alpha \partial_{\bar{\beta}} K$ is given by

$$g_{\psi\bar{\psi}} \sim \psi\bar{\psi}, \quad g_{\psi\bar{\phi}} \sim \psi\bar{\psi}^2\bar{\phi}, \quad g_{\phi\bar{\psi}} \sim \psi^2\bar{\psi}\bar{\phi}, \quad g_{\phi\bar{\phi}} \sim 1.$$

This is consistent with our expectations - at the Landau-Ginzburg point $\psi = \phi = 0$ the metric becomes singular. The curvature 2-form \mathcal{R} and the Chern class c_2 may be calculated straightforwardly from the full expressions for the metric using a symbolic algebra program. Evaluating the Ashok-Douglas density, we find it has leading behaviour

$$d\mu \sim g_{\tau\bar{\tau}} d\tau \wedge d\bar{\tau} \wedge \psi\bar{\psi} d\psi \wedge d\bar{\psi} \wedge d\phi \wedge d\bar{\phi}.$$

The regions on which we compare the Ashok-Douglas formula to our empirical results are balls in ψ and ϕ space. We then expect as leading behaviour

$$\begin{aligned} N(\text{vacua s.t. } |\psi| < r_1) &\sim r_1^4, \\ N(\text{vacua s.t. } |\phi| < r_2) &\sim r_2^2. \end{aligned}$$

To test this expectation, we generated random fluxes and sought solutions of equations (35) to (37) using a numerical root finder. The range of fluxes used was $(-20, 20)$. This is not as large as one might prefer. However, a larger range of fluxes resulted in solutions being produced insufficiently rapidly for our purposes. In order to be able to trust our truncation of the power series, we only kept solutions satisfying

$$\left| \frac{864\psi^6}{\phi \pm 1} \right| < 0.5 \text{ and } |\phi| < 0.75. \quad (38)$$

When processing the numerical results, there is an important subtlety we must account for⁴. It is well known that there is an exact $SL(2, \mathbb{Z})$ symmetry of type IIB,

$$\tau \rightarrow \frac{a\tau + b}{c\tau + d}, \quad \begin{pmatrix} F_3 \\ H_3 \end{pmatrix} \rightarrow \begin{pmatrix} a & b \\ c & d \end{pmatrix} \begin{pmatrix} F_3 \\ H_3 \end{pmatrix}.$$

where $a, b, c, d \in \mathbb{Z}$ and $ad - bc = 1$. Thus each vacuum found has many physically equivalent $SL(2, \mathbb{Z})$ copies that we should not double-count. One way to deal with this would be to fix the gauge explicitly and then perform the Monte-Carlo analysis. Our approach is instead to weight each vacuum by the inverse of the number of copies it has within the sampled flux range. The purpose of this is to ensure that vacua with many $SL(2, \mathbb{Z})$ copies are not preferred.

As well as the $SL(2, \mathbb{Z})$ symmetry, there is a monodromy near the Landau-Ginzburg point that needs similar treatment. From the definition of the periods

⁴We thank S. Kachru for bringing this to our attention.

(30), we can that they have a monodromy under $(\psi, \phi) \rightarrow (\alpha\psi, -\phi)$, where $\alpha^{12} = 1$, of

$$\varpi(\psi, \phi) \rightarrow a \cdot \varpi(\psi, \phi),$$

where

$$a = \begin{pmatrix} 0 & 1 & 0 & 0 & 0 & 0 \\ 0 & 0 & 1 & 0 & 0 & 0 \\ 0 & 0 & 0 & 1 & 0 & 0 \\ 0 & 0 & 0 & 0 & 1 & 0 \\ 0 & 0 & 0 & 0 & 0 & 1 \\ -1 & 0 & 0 & 0 & 0 & 0 \end{pmatrix}.$$

In the symplectic basis, the monodromy matrix A is given by $m \cdot a \cdot m^{-1}$. The effect of this monodromy is to produce a family of physically equivalent solutions related by

$$\begin{aligned} (\psi, \phi) &\rightarrow (\alpha^{-1}\psi, -\phi), \\ f &\rightarrow f \cdot A, \\ h &\rightarrow h \cdot A. \end{aligned} \tag{39}$$

When weighting vacua we need to find the total number of copies lying within the sampled flux range from all symmetries and monodromies. This has important systematic effects as vacua with smaller values of f_i and h_i , and thus smaller values of N_{flux} , have more copies. A naive counting that neglects the symmetries or monodromies that are present thus places undue emphasis on vacua with smaller values of N_{flux} .

We looked at the distribution of vacua within fixed balls in ψ and ϕ space. In figure 1 we plot the number of vacua satisfying (38) and having $|\psi| < r$. The results are seen to agree well with the theoretical prediction. Likewise, figure 2 shows the distribution of vacua for a ball $|\phi| < r$ in ϕ space. The continuous line again represents the cumulative number of vacua and the dots the rescaled numerical integration of $\int_{|\phi| < r} d\mu$. The empirical results are again well captured by the theoretical prediction. Finally, in figure 3 we examine the dependence of the number of vacua on the distance in flux space $N_{flux} = f^T \cdot \Sigma \cdot h$. The graph is fit by $N \sim L^{4.3}$. This is surprising, as the expected scaling is L^6 . Furthermore, in the vicinity of the Landau-Ginzburg point for an analogous one-modulus example, the correct L^4 scaling is found[27]. As we will discuss further in section 4, we believe our results are an artifact of the small flux range used, and that were a larger flux range used we would obtain the correct scaling. As we will shortly describe, in the vicinity of the conifold locus we do obtain the expected scaling with a flux range of $(-40, 40)$.

It is also of interest to study the supersymmetry breaking scale, as measured by $\alpha'^2(2\pi)^4 e^K |W|^2$, for vacua in the vicinity of $\psi = \phi = 0$. This is shown in figure 4. The most noticeable thing about this graph is that the distribution of

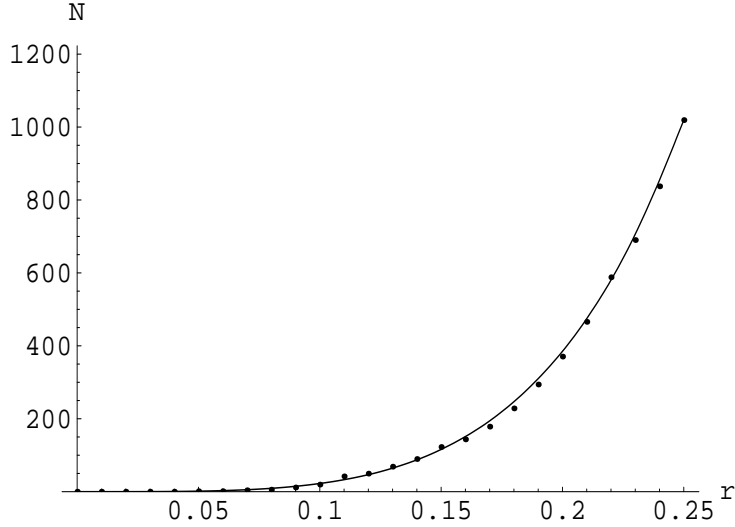


Figure 1: Number of vacua with $|\psi| < r$. The value of N plotted includes a weighting due to the $SL(2, \mathbb{Z})$ copies of each vacuum within the range of fluxes sampled. The dots represent the numerical results, and the continuous line the (rescaled) numerical integration of $\int_{|\psi| < r} d\mu$, where $d\mu$ is the index density. The flux range used was $(-20, 20)$.

the susy breaking scale is uniform near the origin and that the vast majority of vacua therefore have a high supersymmetry breaking scale. We can also observe from the structure of the graph that arbitrarily small values of the gravitino mass should exist as well as supersymmetric solutions. In reference [22], explicit supersymmetric vacua were obtained for this model.

3.2 The Vicinity of the Conifold Locus

The Calabi-Yau \mathcal{M} has a codimension one conifold degeneration along the moduli space locus $864\psi^6 + \phi = 1$. The moduli space curvature diverges near a conifold point and the expectation is that vacua should cluster near the conifold locus.

To study these vacua numerically, we must restrict attention to a small region of the conifold locus where we can compute the periods explicitly. We take this region to be the neighbourhood of the point $\phi = 0, \psi = \psi_0 = 864^{-\frac{1}{6}}$. If we write $\psi = \psi_0 + \xi$ and truncate the periods at first order in ξ and ϕ , then $\Pi(\xi, \phi) = (\mathcal{G}_1, \mathcal{G}_2, \mathcal{G}_3, z_1, z_2, z_3)$ is approximated by

$$\begin{aligned}
\mathcal{G}_1 &= 3202\xi + 171.8\phi + \mathcal{O}(\xi^2, \phi^2, \xi\phi) \\
\mathcal{G}_2 &= 4323 - i(1553\xi + 107.4\phi) + \mathcal{O}(\xi^2, \phi^2, \xi\phi) \\
\mathcal{G}_3 &= (-492.7 + 1976.8i) + (371.0 - 300.2i)\xi + (-259.0 - 59.0i)\phi + \mathcal{O}(\xi^2, \phi^2, \xi\phi) \\
z_1 &= \frac{-1}{2\pi i} \mathcal{G}_1 \ln(\mathcal{G}_1) + 784.8i - 2306i\xi - 44.35i\phi + \mathcal{O}(\xi^2, \phi^2, \xi\phi)
\end{aligned}$$

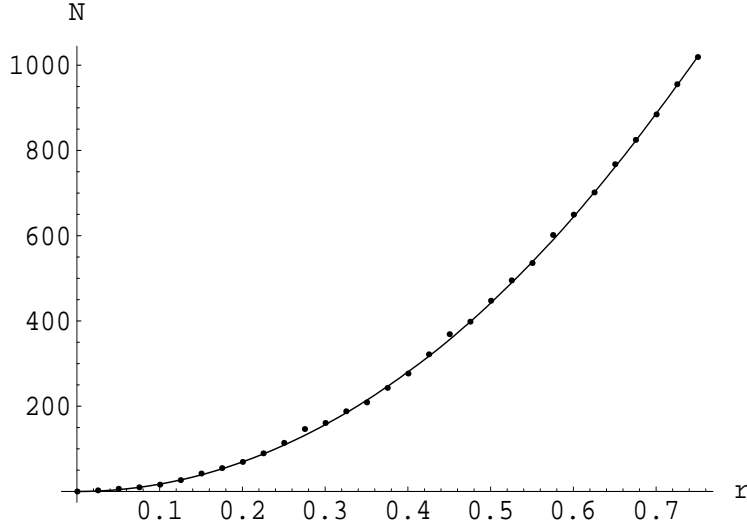


Figure 2: The weighted number of vacua, N , with $|\phi| < r$. The dots represent the numerical results and the continuous line the numerical integration of $\int_{|\phi| < r} d\mu$, rescaled by the same factor as in diagram 1.

$$\begin{aligned}
z_2 &= (-994.6 - 184.8i) + (861.9 + 476.5i)\xi + (9.91 - 112.7i)\phi + \mathcal{O}(\xi^2, \phi^2, \xi\phi) \\
z_3 &= i(369.5 - 953.0\xi + 225.4\phi) + \mathcal{O}(\xi^2, \phi^2, \xi\phi)
\end{aligned} \tag{40}$$

The numerical values were found by evaluating the series (28) up to one hundred terms in ψ and twenty-five terms in ϕ . The values for the coefficients of the $\mathcal{O}(\xi, \phi)$ terms were sensitive to the number of terms used in the power series at the level of a couple of percentage points. We did not keep terms quadratic in ξ and ϕ - inclusion of these would lead to $\mathcal{O}(\xi)$ corrections to the results below.

The general form of the periods is standard. The cycles corresponding to $\mathcal{G}_2, \mathcal{G}_3, z_2$ and z_3 are all remote from the conifold singularity, resulting in the associated periods being both regular and non-vanishing near the conifold degeneration. Recalling that the conifold is a cone with a base that is topologically $S^2 \times S^3$, the cycle corresponding to G_1 is the S^3 that shrinks to zero size along the conifold locus. The period along this cycle is regular near the conifold locus and vanishing along it. Finally, the cycle corresponding to z_1 is that dual to the S^3 . It is therefore not uniquely defined and is in fact well known to have a monodromy under a loop around the conifold locus. Its period takes the form $(-\frac{1}{2\pi i}\mathcal{G}_1 \ln(\mathcal{G}_1) + \text{analytic terms})$.

It is convenient to define $Z = (\frac{3202}{171.8})\xi + \phi$ and rewrite the periods as

$$\begin{aligned}
\mathcal{G}_1 &= 171.8 Z, \\
\mathcal{G}_2 &= 4323 + 107.4i Z - 3554i \xi, \\
\mathcal{G}_3 &= 784.8 - (259 + 59i) Z + (5198 + 799i) \xi,
\end{aligned}$$

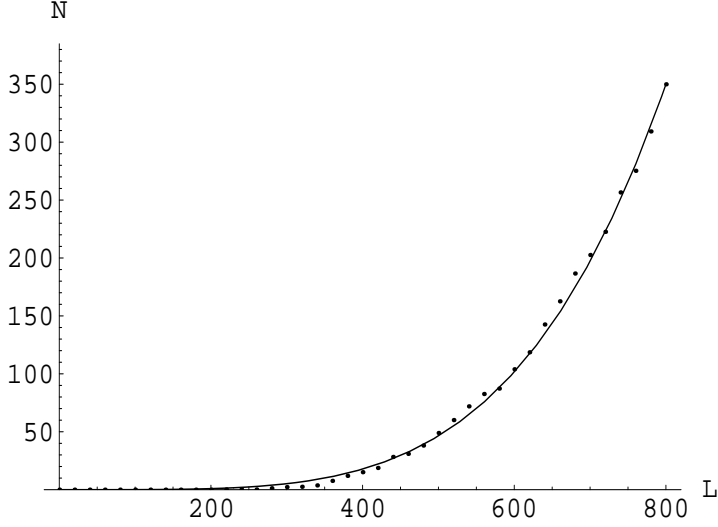


Figure 3: The weighted number of vacua N with $N_{flux} < L$. 4.5×10^6 sets of fluxes were generated, with values of L equally distributed between 0 and 800 and the range of fluxes being $(-20, 20)$. The results are fit by $N \sim L^{4.3}$.

$$\begin{aligned}
z_1 &= \frac{-1}{2\pi i} 171.8 Z \ln(Z) + 784.8 - 44.4i Z - 1479i \xi, \\
z_2 &= (-994.6 - 184.8i) + (9.91 - 112.7i) Z + (677 + 2577i) \xi, \\
z_3 &= i(369.5 + 225.4 Z - 5154 \xi).
\end{aligned} \tag{41}$$

Z is a measure of the distance from the conifold locus. We are interested in vacua extremely close to the conifold locus - typically $\ln|Z| < -5$ - and thus we will regard $|Z| \ll |\xi| \ll 1$. Having set up the periods (41), we can now compute the Ashok-Douglas expectation for the index density and compare this with numerical results.

Let us now solve equations (20). First,

$$D_\tau W = 0 \Rightarrow (f - \bar{\tau}h) \cdot \Pi = 0 \Rightarrow \tau = \frac{f \cdot \Pi^\dagger}{h \cdot \Pi^\dagger}. \tag{42}$$

This can be written as

$$\tau = \frac{a_0 + a_1 \bar{\xi}}{b_0 + b_1 \bar{\xi}} + \mathcal{O}(Z \ln Z), \tag{43}$$

where a_i and b_i are flux-dependent quantities. Next,

$$D_\xi W = 0 \Rightarrow (f - \tau h) \cdot (c_0 + c_1 \xi + c_2 \bar{\xi} + \mathcal{O}(\xi^2)) = 0. \tag{44}$$

Using (43) this becomes a linear equation for ξ , easily solved to determine ξ and τ . We finally need the value of $\ln Z$. This is obtained by considering

$$D_Z W = 0 \Rightarrow (f_4 - \tau h_4) \ln Z = (d_0 + d_1 \tau) + (d_2 + d_3 \tau) \xi + (d_4 + d_5 \tau) \bar{\xi} \tag{45}$$

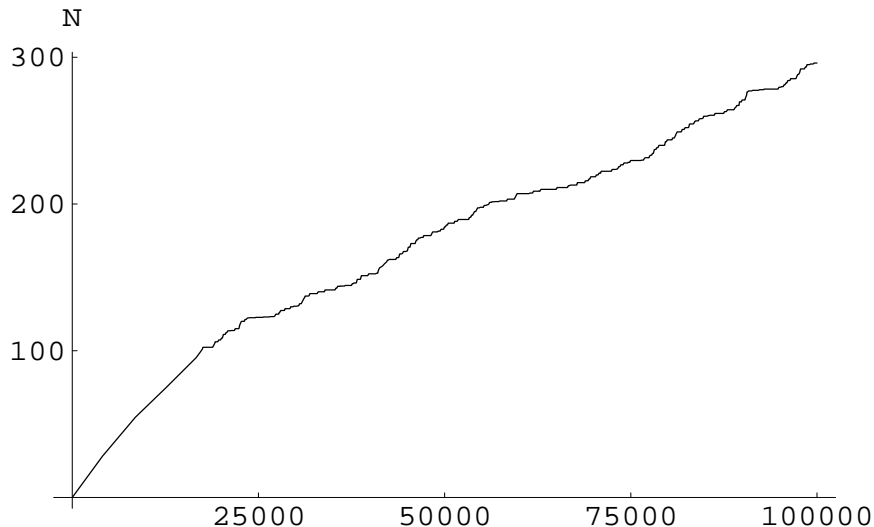


Figure 4: The value of $(2\pi)^4 e^K |W|^2$ in units of $(\alpha')^2$ for vacua in the vicinity of $\psi = \phi = 0$, for $(2\pi)^4 e^K |W|^2 < 100000$. The flux range was $(-20, 20)$, and the vacua satisfied the conditions (38).

Substituting in for τ and ξ from (43) and (44) then gives the value of $\ln Z$.

When analysing the results we must account for the $SL(2, \mathbb{Z})$ copies discussed in section 3.1. There is also a monodromy near the conifold. When solving for $\ln Z$, we impose no restriction on the imaginary part of $\ln Z$. There is then a monodromy

$$\begin{aligned}
 \ln Z &\rightarrow \ln Z + 2\pi i, \\
 (f_1, f_2, f_3, f_4, f_5, f_6) &\rightarrow (f_1 + f_4, f_2, f_3, f_4, f_5, f_6), \\
 (h_1, h_2, h_3, h_4, h_5, h_6) &\rightarrow (h_1 + h_4, h_2, h_3, h_4, h_5, h_6).
 \end{aligned} \tag{46}$$

corresponding to a loop in moduli space around the conifold locus. This gives a further source of physically equivalent solutions that should not be double-counted. For each vacuum, we then count the total number of copies within the specified flux range and weight by the inverse of this number.

Results are shown below. In figure 5 we show the clustering of vacua by plotting the distribution of vacua transverse to the conifold locus. A similar plot of vacua parallel to the conifold locus shows no such clustering, indicating that there is no preferred position along the conifold locus. In figure 6 we perform a quantitative comparison with the expected vacuum density, finding very good agreement over a large range of values of $\ln Z$. In figure 7 we examine the scaling with L of the number of vacua having $N_{flux} < L$. This reproduces the expected L^6 scaling of (21). We also computed the susy breaking scale, $\alpha'^2 (2\pi)^4 e^K |W|^2$. The distribution of susy breaking scales is plotted in figure 8, and is uniform near zero.

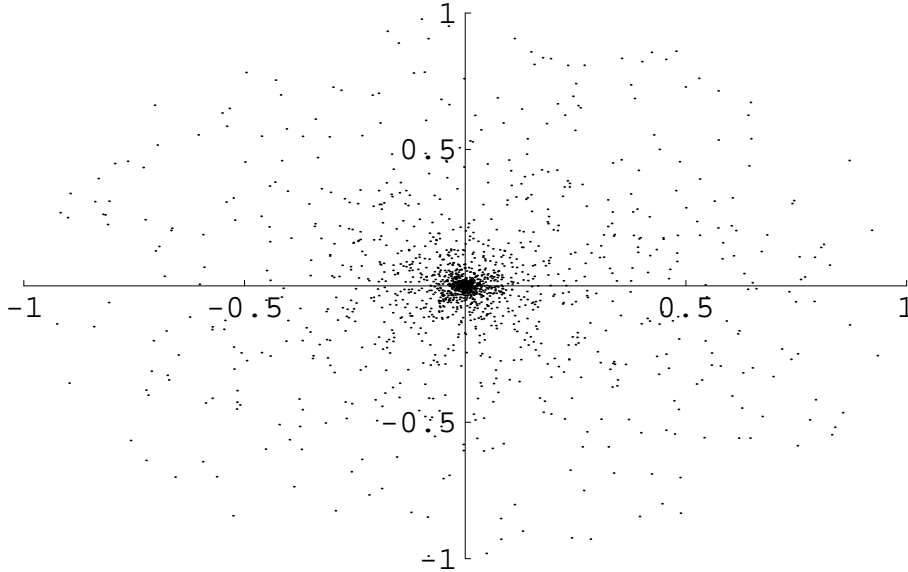


Figure 5: The value of Z for vacua near the conifold. We have restricted to $|Z| < 0.0001$ and have rescaled the above plot by 10^4 . The flux range used was $(-40,40)$.

4 Summary and Discussion

Let us briefly summarise our results.

1. We constructed a large class of flux vacua for the two-moduli Calabi-Yau threefold $\mathbb{P}^4_{[1,1,2,2,6]}$. We independently computed the Ashok-Douglas density and compared with our results. We find good agreement which improves as the range of fluxes is increased. The number of vacua was limited mostly by working in two patches in moduli space: the region near $\psi = \phi = 0$ and the region close to the conifold singularity $\phi + 864\psi^6 = \pm 1$.
2. We found a large concentration of vacua close to the conifold singularity as predicted, with the detailed distribution of the vacua being in close accordance with expectation.
3. In both regions, the values of the superpotential are uniformly distributed near zero. As a consequence, large values of the superpotential, corresponding to a large supersymmetry breaking scale, are more abundant than small ones.
4. In both regions the number of models scaled as a power of the maximum permitted value of N_{flux}, L_{max} . In the vicinity of the conifold we reproduced the expected L^6 scaling. In the region close to the Landau-Ginzburg point

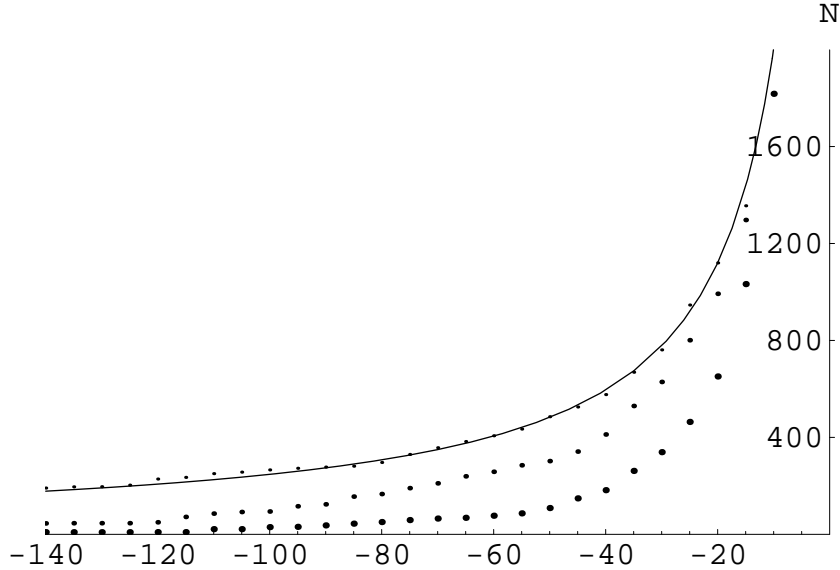


Figure 6: The distribution of vacua transverse to the conifold. We plot the number of vacua having $\ln Z < D$ for $D \in (-120, -5)$ against D , restricting to $|\xi| < 0.05$. The dots refer to the vacua found numerically and the smooth line to the Ashok-Douglas prediction. We include results for three flux ranges - $(-20, 20)$, $(-30, 30)$ and $(-40, 40)$. The fit of the results to the expected distribution improves markedly as the flux range is increased.

we only achieved an scaling as $L^{4.3}$. We attribute the failure to achieve the expected scaling in this region to the smaller range of fluxes used there.

An important feature of our analysis is that the flux range used has a significant effect on the results. If the flux range is insufficiently large, then the distribution of vacua found numerically will not fit with the theoretical density. This is most strikingly illustrated for the case of the conifold in figure 6. Similar behaviour was seen for the scaling of the number of vacua with L - in the vicinity of the conifold locus, a reduction of the flux range to $(-20, 20)$ caused a reduction in the power of the scaling from ≈ 6 to ≈ 5 . Given this, we believe that the scaling of $N(\text{vacua} | N_{flux} < L) \sim L^{4.3}$ found in the vicinity of the Landau-Ginzburg point is simply an artefact of the flux range used.

We can see a similar dependence on the range of fluxes used in the distribution of the dilaton. After being transformed to the $SL(2, \mathbb{Z})$ fundamental region, the expectation from equation (22) is that the number of vacua with $\text{Im}(\tau) > \tau_0$ should scale like $\frac{1}{\tau_0}$. In figure 9 we compare this with numerical results arising from using flux ranges $(-20, 20)$, $(-40, 40)$ and $(-60, 60)$.

We see that as the flux range increases the empirical distribution tends towards the theoretical one, and also that even with a flux range of $(-60, 60)$ the two distributions do not yet fully match. In general terms these results are reas-

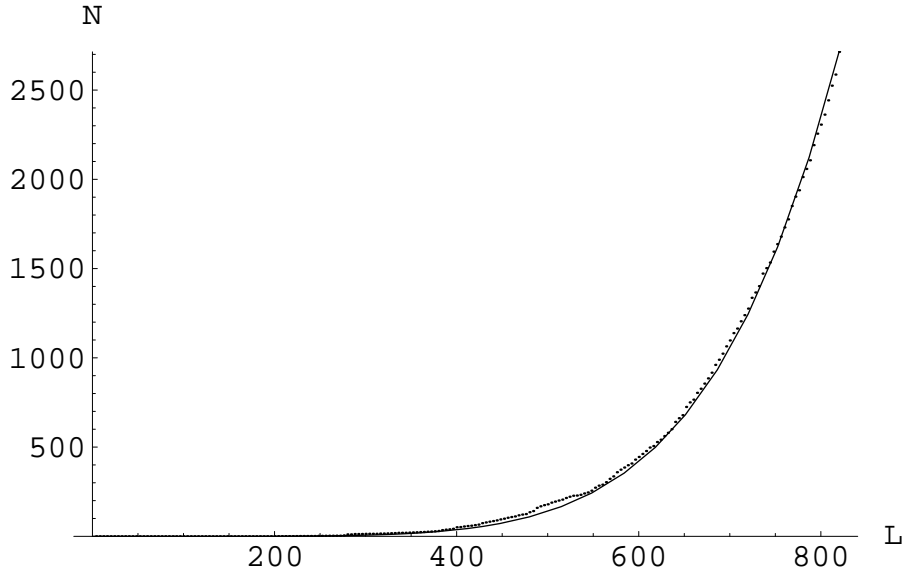


Figure 7: The weighted number of vacua with $N_{\text{flux}} < L$. The curve is fit well by $N \propto L^6$. The range of fluxes used was $(-40,40)$.

suring in the sense that arbitrarily large values of the dilaton can be obtained, consistent with the weak coupling approximation although they are not statistically preferred.

As we have concentrated on only two complex structure moduli from a total of 128, we have explored only a minuscule sample of the full set of flux vacua for this model. Still, we obtained sufficient statistics to see the expected distribution of vacua. There is a clear computational obstruction to exploring the full spectrum of models for a given Calabi-Yau. However, we have seen that the consistency requirements of small string coupling and large volume are largely disfavoured statistically. The relevant class of vacua will then be suppressed compared to the large estimated totals of order 10^{100} . Nonetheless, given this large number it is reasonable to expect many solutions with very small values of the supersymmetry breaking scale (which in the KKLT scenario becomes the large volume constraint). It would be desirable to develop techniques that, rather than simply counting the number of vacua by numerically scanning the parameter space, select only those which satisfy the consistency and phenomenological requirements. Some small values of $|W|$ can be found explicitly - [22] contains an example where $|W| \approx 4 \times 10^{-3}$ and the first reference of [30] a case where $|W|^2 \approx 2 \times 10^{-4}$. The efficient discovery of phenomenologically acceptable vacua is harder; the techniques recently developed in [28] may be of use in this regard. Finally, let us note that in our study of this model we have addressed neither the issue of soft supersymmetry breaking terms induced solely by the fluxes nor the non-perturbative superpotential required to complete the moduli fixing and lift the

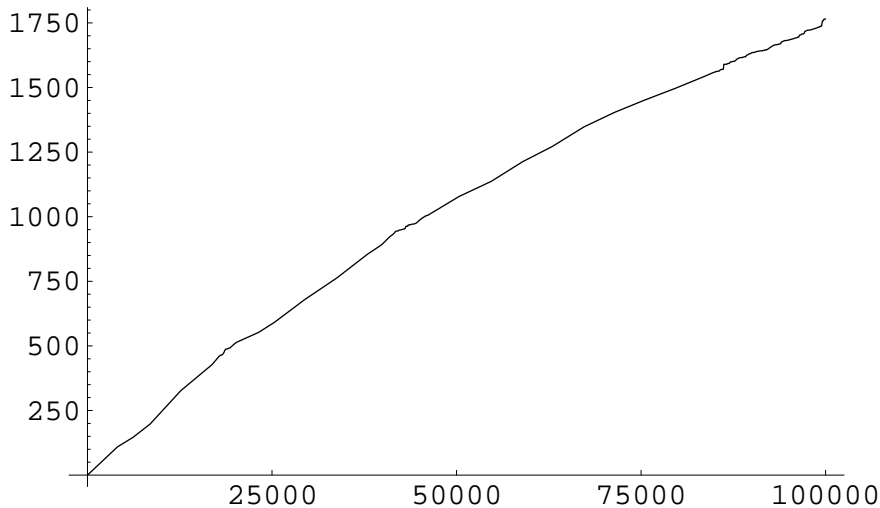


Figure 8: The value of $(2\pi)^4 e^K |W|^2$ in units of $(\alpha')^2$ for vacua near the conifold, for $(2\pi)^4 e^K |W|^2 < 100000$. The flux range was $(-40, 40)$ and we restricted to vacua satisfying $|\xi| < 0.05$.

potential to get de Sitter space as in the KKLT scenario. For recent progress in these directions, [29, 30] may be consulted.

Let us finish with a general observation. The Calabi-Yau considered here has $h^{1,1} = 2$ and $h^{2,1} = 128$. We have turned on fluxes along the cycles corresponding to only two of the 128 complex structure moduli. We would expect that some of the remaining moduli should be frozen out by the orientifold symmetry, but it would still be obviously impractical to attempt either to write down or to solve the moduli stabilisation equations with all fluxes turned on. However, if we assume that the Ashok-Douglas density remains valid then we can say something about the generic situation. Suppose we have K cycles supporting flux and that - as holds for this and many other F-theory models -

$$N_{D3} + N_{flux} = L_{max} \sim 1000. \quad (47)$$

The Ashok-Douglas density (21) tells us that

$$N(\text{vacua} | N_{flux} < L_*) \sim L_*^K. \quad (48)$$

The fraction of vacua having $N_{D3} \geq n$ is then estimated by

$$\frac{N(\text{vacua} | N_{flux} \leq L_{max} - n)}{N(\text{vacua} | N_{flux} \leq L_{max})} = \frac{(L_{max} - n)^K}{L_{max}^K}. \quad (49)$$

For $K \sim 200$, then for $n = 5$ this is approximately $\frac{1}{e} \approx 0.36$. We then see that despite the large amount of $D3$ -brane charge we have to play with, generic

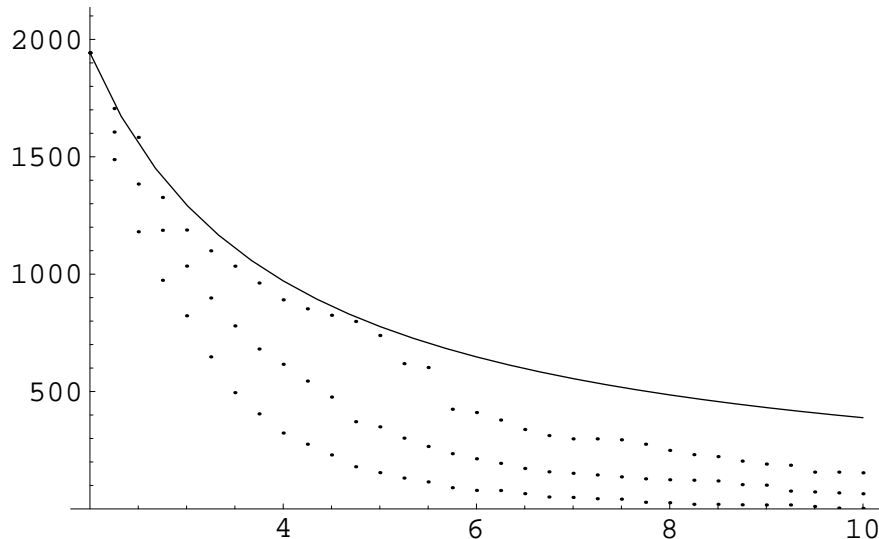


Figure 9: Distribution of vacua near the conifold locus with $\text{Im}(\tau) > y$ for $y \in (2, 10)$. Results have been brought to the same scale and plotted for three separate flux ranges: $(-20, 20)$, $(-40, 40)$ and $(-60, 60)$. We see that as the flux range increases the empirical plot moves closer to the expected result (represented by a smooth line).

vacua have rather small gauge groups ⁵. This is appealing from a phenomenological point of view if the standard model were to live on D3 branes as in the realistic models of [32]. Of course, the actual numbers depend on the particular Calabi-Yau, the number of 3-cycles surviving the orientifold projection and the modifications to the Ashok-Douglas density when $L \approx (\text{a few})K$, but the general conclusion should be broadly unaffected. Clearly, there is no reason to require that our universe belong to statistically preferred classes of vacua, but given the discussion above, it is always useful to know which properties are generic and which are not.

Acknowledgements

We would like to thank M. Douglas, A. Giryavets and particularly S. Kachru for very useful suggestions, comments and discussions. We are also grateful for interesting conversations with P. Berglund, X. de la Ossa, A. Font, D. Grellscheid

⁵This discussion has to be modified when including the D3 brane moduli which, when fixed, will contribute to the statistics of vacuum degeneracy. Probably arguments using the attractor mechanism towards enhanced symmetry points [31] can be used to control this extra degeneracy. A more detailed analysis of this issue is beyond the scope of this note. We thank E. Dudas and S. Kachru for discussions on these points.

and K. Suruliz. FQ thanks the Aspen Center for Physics for hospitality during its summer workshop ‘Strings and the Real World’, where part of this project was developed. JC thanks EPSRC for a research studentship. FQ is partially supported by PPARC and a Royal Society Wolfson award.

References

- [1] J. Polchinski, *What is string theory?*, arXiv:hep-th/9411028; *String duality: A colloquium*, Rev. Mod. Phys. **68** (1996) 1245 [arXiv:hep-th/9607050].
- [2] For recent overall reviews see for instance: F. Quevedo, “Phenomenological Aspects of D-branes” in *Trieste 2002, Superstrings and related matters* 232-330; E. Kiritsis, “D-branes in standard model building, gravity and cosmology,” Fortsch. Phys. **52** (2004) 200 [arXiv:hep-th/0310001].
- [3] For recent reviews with many references see for instance: F. Quevedo, “Lectures on string / brane cosmology,” Class. Quant. Grav. **19** (2002) 5721 [arXiv:hep-th/0210292]; A. Linde, “Prospects of inflation,” arXiv:hep-th/0402051; C. P. Burgess, “Inflatable string theory?,” arXiv:hep-th/0408037.
- [4] K. Kikkawa and M. Yamasaki, “Casimir Effects In Superstring Theories,” Phys. Lett. B **149** (1984) 357; N. Sakai and I. Senda, “Vacuum Energies Of String Compactified On Torus,” Prog. Theor. Phys. **75** (1986) 692 [Erratum-ibid. **77** (1987) 773].
- [5] P. Candelas, M. Lynker and R. Schimmrigk, “Calabi-Yau Manifolds In Weighted P(4),” Nucl. Phys. B **341** (1990) 383; B. R. Greene and M. R. Plesser, “Duality In Calabi-Yau Moduli Space,” Nucl. Phys. B **338** (1990) 15.
- [6] A. Font, L. E. Ibanez, D. Lust and F. Quevedo, “Strong - Weak Coupling Duality And Nonperturbative Effects In String Theory,” Phys. Lett. B **249** (1990) 35. C. M. Hull and P. K. Townsend, “Unity of superstring dualities,” Nucl. Phys. B **438** (1995) 109 [arXiv:hep-th/9410167]; E. Witten, “String theory dynamics in various dimensions,” Nucl. Phys. B **443** (1995) 85 [arXiv:hep-th/9503124].
- [7] C. M. Hull, “Superstring Compactifications With Torsion And Space-Time Supersymmetry,” Print-86-0251 (CAMBRIDGE). Turin Superunification (1985) 347; A. Strominger, “Superstrings With Torsion,” Nucl. Phys. B **274** (1986) 253. S. Sethi, C. Vafa and E. Witten, “Constraints on low-dimensional string compactifications,” Nucl. Phys. B **480** (1996) 213 [hep-th/9606122]; J. Polchinski and A. Strominger, “New Vacua for Type II String Theory,”

- Phys. Lett. B **388** (1996) 736 [arXiv:hep-th/9510227]; K. Dasgupta, G. Rajesh and S. Sethi, “M theory, orientifolds and G-flux,” JHEP **9908** (1999) 023 [hep-th/9908088]. S. Kachru, M. B. Schulz and S. Trivedi, “Moduli stabilization hep-th/0201028.
- [8] S. B. Giddings, S. Kachru and J. Polchinski, “Hierarchies from fluxes in string compactifications,” Phys. Rev. **D66**, 106006 (2002);
- [9] S. Kachru, R. Kallosh, A. Linde and S. P. Trivedi, “De Sitter vacua in string theory,” Phys. Rev. D **68** (2003) 046005 [arXiv:hep-th/0301240].
- [10] For recent reviews see: V. Balasubramanian, “Accelerating universes and string theory,” Class. Quant. Grav. **21** (2004) S1337 [arXiv:hep-th/0404075]; E. Silverstein, “TASI / PiTP / ISS lectures on moduli and microphysics,” arXiv:hep-th/0405068.
- [11] C. Escoda, M. Gomez-Reino and F. Quevedo, “Saltatory de Sitter string vacua,” JHEP **0311** (2003) 065 [arXiv:hep-th/0307160].
- [12] C. P. Burgess, R. Kallosh and F. Quevedo, “de Sitter string vacua from supersymmetric D-terms,” JHEP **0310** (2003) 056 [arXiv:hep-th/0309187].
- [13] A. Saltman and E. Silverstein, “The scaling of the no-scale potential and de Sitter model building,” arXiv:hep-th/0402135.
- [14] M. R. Douglas, “The statistics of string / M theory vacua,” JHEP **0305**, 046 (2003) [arXiv:hep-th/0303194]. For a recent overview see: M. R. Douglas, “Brief results in vacuum statistics,” [arXiv:hep-th/0409207].
- [15] S. Ashok and M. R. Douglas, “Counting flux vacua,” JHEP **0401**, 060 (2004) [arXiv:hep-th/0307049].
- [16] F. Denef and M. R. Douglas, “Distributions of flux vacua,” JHEP **0405**, 072 (2004) [arXiv:hep-th/0404116].
- [17] A. Giriyavets, S. Kachru and P. K. Tripathy, “On the taxonomy of flux vacua,” JHEP **0408**, 002 (2004) [arXiv:hep-th/0404243].
- [18] P. Candelas, X. C. De La Ossa, P. S. Green and L. Parkes, “A Pair Of Calabi-Yau Manifolds As An Exactly Soluble Superconformal Theory,” Nucl. Phys. B **359** (1991) 21.
- [19] P. Berglund, P. Candelas, X. De La Ossa, A. Font, T. Hubsch, D. Jancic and F. Quevedo, “Periods for Calabi-Yau and Landau-Ginzburg vacua,” Nucl. Phys. B **419**, 352 (1994) [arXiv:hep-th/9308005].

- [20] P. Candelas, X. De La Ossa, A. Font, S. Katz and D. R. Morrison, “Mirror symmetry for two parameter models. I,” Nucl. Phys. B **416**, 481 (1994) [arXiv:hep-th/9308083].
- [21] A. Misra and A. Nanda, “Flux vacua statistics for two-parameter Calabi-Yau’s,” arXiv:hep-th/0407252.
- [22] A. Giriyavets, S. Kachru, P. K. Tripathy and S. P. Trivedi, “Flux compactifications on Calabi-Yau threefolds,” JHEP **0404**, 003 (2004) [arXiv:hep-th/0312104].
- [23] A. Sen, “Orientifold limit of F-theory vacua,” Phys. Rev. D **55**, 7345 (1997) [arXiv:hep-th/9702165].
- [24] S. Gukov, C. Vafa and E. Witten, “CFT’s from Calabi-Yau fourfolds,” Nucl. Phys. B **584**, 69 (2000) [Erratum-ibid. B **608**, 477 (2001)] [arXiv:hep-th/9906070].
- [25] P. Candelas and X. de la Ossa, “Moduli Space Of Calabi-Yau Manifolds,” Nucl. Phys. B **355** (1991) 455.
- [26] A. Giriyavets and S. Kachru, private communication.
- [27] O. DeWolfe, A. Giriyavets, S. Kachru and W. Taylor, to appear.
- [28] B. C. Allanach, D. Grellscheid and F. Quevedo, “Genetic algorithms and experimental discrimination of SUSY models,” JHEP **0407** (2004) 069 [arXiv:hep-ph/0406277].
- [29] P. G. Camara, L. E. Ibanez and A. M. Uranga, “Flux-induced SUSY-breaking soft terms,” Nucl. Phys. B **689** (2004) 195 [arXiv:hep-th/0311241]; “Flux-induced SUSY-breaking soft terms on D7-D3 brane systems,” [arXiv:hep-th/0408036]; M. Grana, T. W. Grimm, H. Jockers and J. Louis, “Soft supersymmetry breaking in Calabi-Yau orientifolds with D-branes and fluxes,” Nucl. Phys. B **690** (2004) 21 [arXiv:hep-th/0312232]; D. Lust, S. Reffert and S. Stieberger, “Flux-induced soft supersymmetry breaking in chiral type IIb orientifolds with D3/D7-branes,” arXiv:hep-th/0406092; H. Jockers and J. Louis, “The effective action of D7-branes in $N = 1$ Calabi-Yau orientifolds,” arXiv:hep-th/0409098.
- [30] F. Denef, M. R. Douglas and B. Florea, “Building a better racetrack,” JHEP **0406** (2004) 034 [arXiv:hep-th/0404257]; D. Robbins and S. Sethi, “A barren landscape,” arXiv:hep-th/0405011; L. Gorlich, S. Kachru, P. K. Tripathy and S. P. Trivedi, “Gaugino condensation and nonperturbative superpotentials in flux compactifications,” arXiv:hep-th/0407130.

- [31] L. Kofman, A. Linde, X. Liu, A. Maloney, L. McAllister and E. Silverstein, “Beauty is attractive: Moduli trapping at enhanced symmetry points,” *JHEP* **0405** (2004) 030 [arXiv:hep-th/0403001]; L. McAllister and I. Mitra, “Relativistic D-brane scattering is extremely inelastic,” arXiv:hep-th/0408085.
- [32] G. Aldazabal, L. E. Ibanez, F. Quevedo and A. M. Uranga, “D-branes at singularities: A bottom-up approach to the string embedding of the standard model,” *JHEP* **0008** (2000) 002 [arXiv:hep-th/0005067]; J. F. G. Cascales, M. P. Garcia del Moral, F. Quevedo and A. M. Uranga, “Realistic D-brane models on warped throats: Fluxes, hierarchies and moduli stabilization,” *JHEP* **0402** (2004) 031 [arXiv:hep-th/0312051].